Arylazopyrazole as photo-switch for controllable self-assembly of pillar[6]arene-based supramolecular amphiphile

Yishu Yu[a], Xiaotian Qu[a], Junran Li[a], Feihe Huang*[b] and Jie Yang*[a]

[a.] College of Science, Nanjing Forestry University, Nanjing, 210037, P.R. China.
E-mail: jieyang@njfu.edu.cn.

[b.] State Key Laboratory of Chemical Engineering, Key Laboratory of Excited-State Materials of Zhejiang Province, Stoddart Institute of Molecular Science, Department of Chemistry, Zhejiang University, Hangzhou 310027, P.R. China. E-mail: fhuang@zju.edu.cn.

Electronic Supplementary Information (19 pages)

1. Materials and methods

All reagents were commercially available and used as supplied without further purification. Solvents were either employed as purchased or dried according to procedures described in the literature. **CWP6** was prepared and purified according to previously published methods.[S1, S2] ^{1}H NMR spectra were recorded on a Bruker AVANCE NEO 400 spectrophotometer using the deuterated solvent as the lock and the residual solvent or TMS as the internal reference. UV-*vis* spectra were taken on a Perkin-Elmer Lambda 950 UV-*vis* spectrophotometer. The path length of the cuvette is 10 mm. The critical aggregation concentration (CAC) values were determined on a DDS-307 instrument. Bright field transmission electron microscopy (TEM) micrographs were obtained with a JEOL 2100Plus microscope operating at 200 kV, equipped with a Gatan OneView IS camera. TEM samples were prepared by drop-coating the solution onto a carbon-coated copper grid. The corresponding solution was left to stand for 5 min and eliminated by a microporous membrane. Dynamic light scattering (DLS) measurements were performed on a goniometer ALV/CGS-3 using a UNIPHASE He-Ne laser operating at 632.8 nm. LED irradiators (5.2 mW cm^{-2} at 365 nm; 7.5 mW cm^{-2} at 520 nm) were used for the photoswitching experiments.

2. *Synthesis*

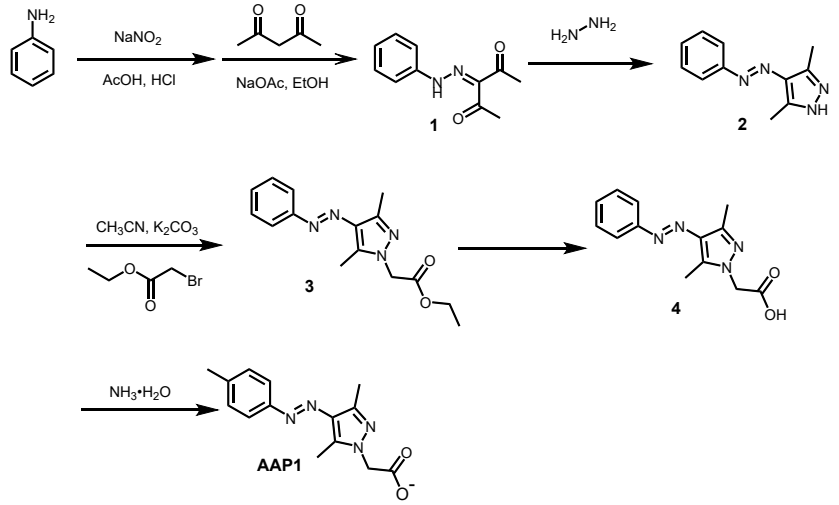

Scheme 1. The synthetic route of compound **AAP1**.

Synthesis of compound **1**: $NaNO_2$ (2.12 g, 30 mmol) dissolved in water was added dropwise to a solution of aniline (2.33 g, 25 mmol) in AcOH (32.5 ml) and HCl (5.75 ml) at 0 ℃ and stirred for 45 minutes. The resulting diazonium salt was transferred to a suspension of pentane-2,4-dione (3.26 g, 32.5 mmol) and NaOAc (6.15g, 75 mmol) in EtOH (25 ml) and water (15 ml) and stirred for 1 hour. Compound **1** was collected by filtration, washed with water thrice and then dried under vacuum (4.44 g, 19 mmol). The ^{1}H NMR spectrum of compound **1** is shown in Figure S1 and the ^{13}C NMR spectrum is shown in Figure S2. ^{1}H NMR (400 MHz, $CDCl_3$, 298 K) δ (ppm): 14.76 (s, 1H), 7.44 (s, 4H), 7.28 (s, 1H), 2.63 (s, 3H), 2.52 (s, 3H). ^{13}C NMR (100 MHz, $CDCl_3$, 298 K) δ (ppm): 197.98, 197.16, 141.55, 133.35, 129.68, 125.92, 116.28, 31.68.

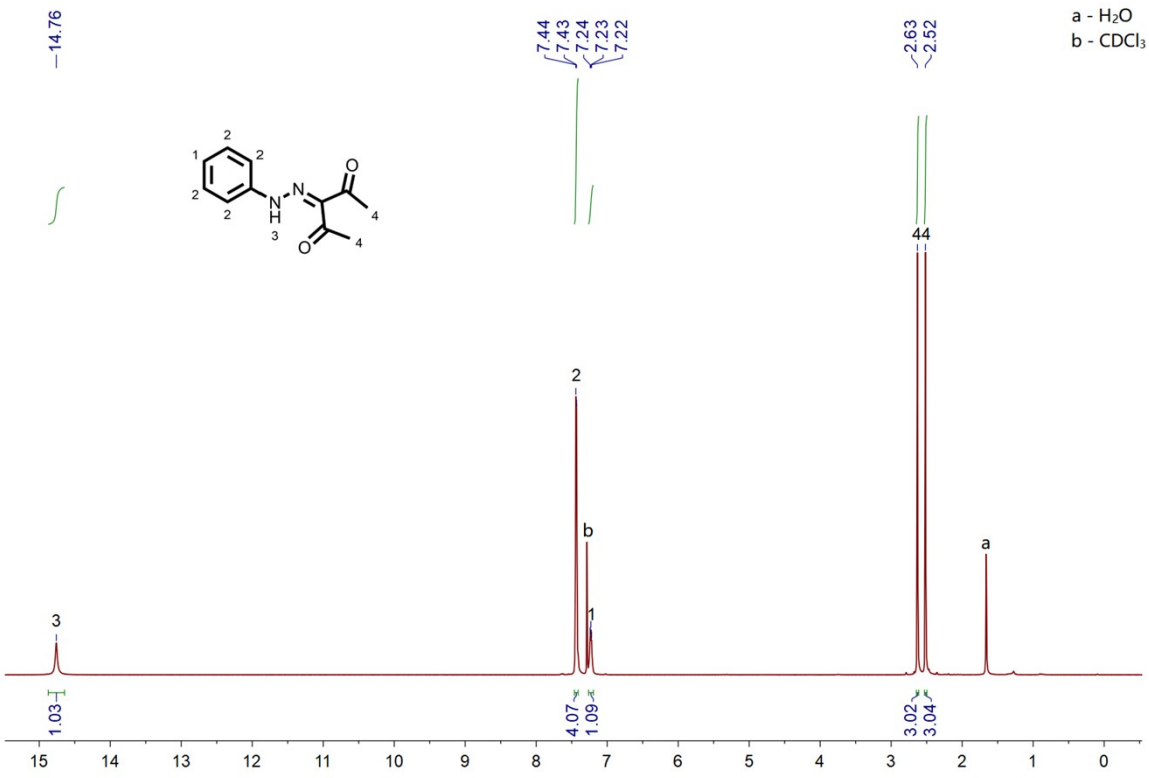

Figure S1. ^{1}H NMR spectrum (400 MHz, $CDCl_3$, 298 K) of compound **1**.

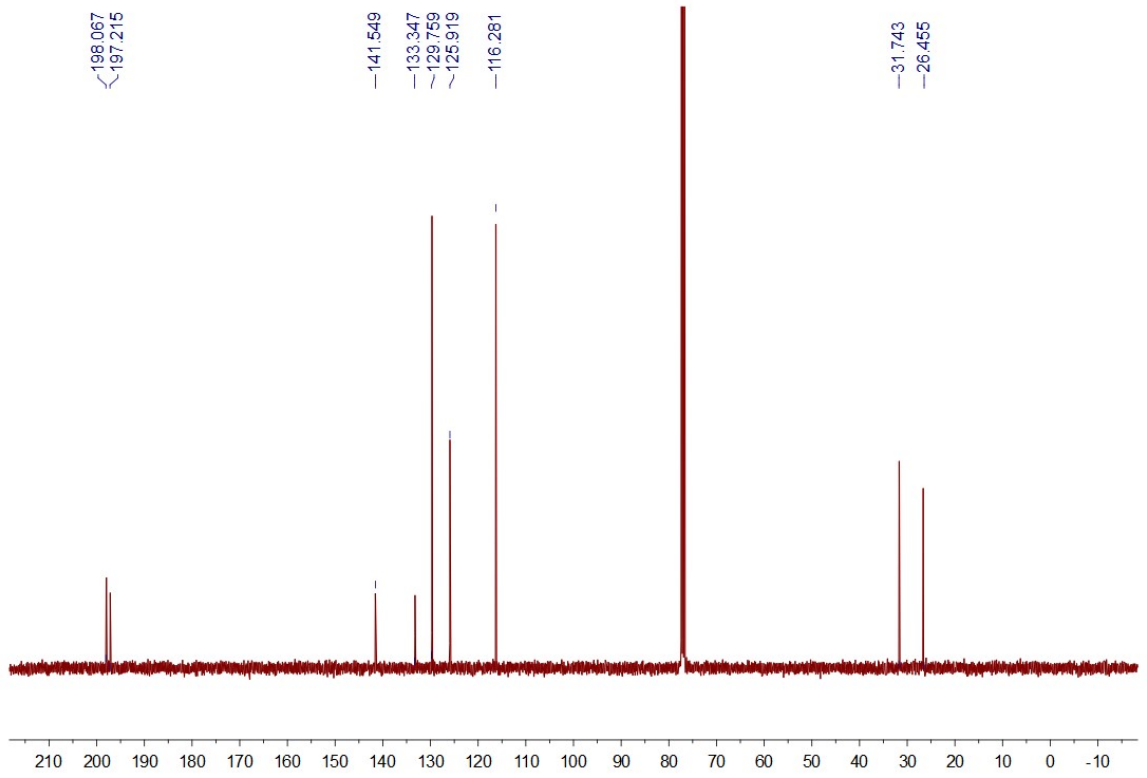

Figure S2. ^{13}C NMR spectrum (100 MHz, $CDCl_3$, 298 K) of compound **1**.

Synthesis of compound **2**: hydrazine hydrate (0.95 g, 19 mmol) was added to a solution of compind **1** in EtOH and refluxed for 3 hours. Concentration under reduced pressure yielded the resulting compound **2** (3.72 g, 18.6 mmol). The ^{1}H NMR spectrum of compound **2** is shown in Figure S3 and the ^{13}C NMR spectrum is shown in Figure S4. ^{1}H NMR (400 MHz, $CDCl_3$, 298 K) δ (ppm): 7.18 (t, J = 7.5 Hz, 2H), 6.78 (t, J = 7.2 Hz, 1H), 6.71 (d, J = 7.6 Hz, 2H), 2.20 (s, 6H). ^{13}C NMR (100 MHz, $CDCl_3$, 298 K) δ (ppm): 129.29, 118.58, 116.75, 115.11, 58.46, 9.90.

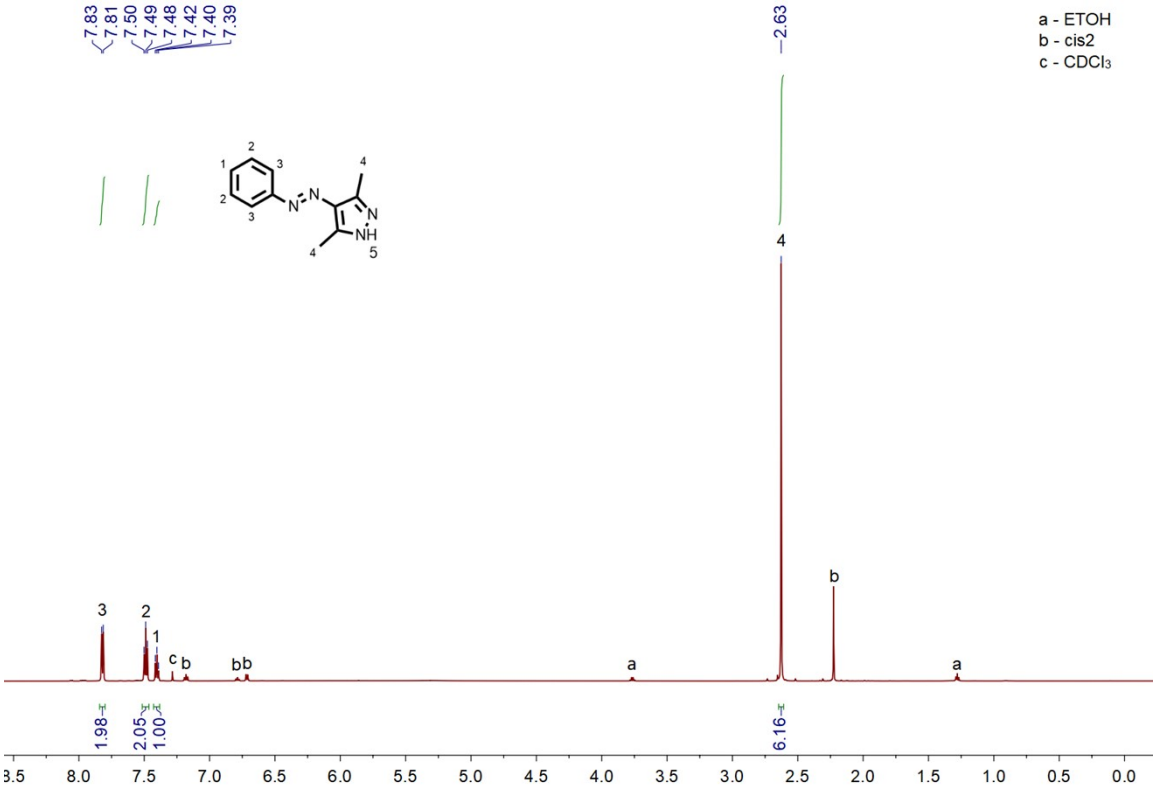

Figure S3. ^{1}H NMR spectrum (400 MHz, $CDCl_3$, 298 K) of compound **2**.

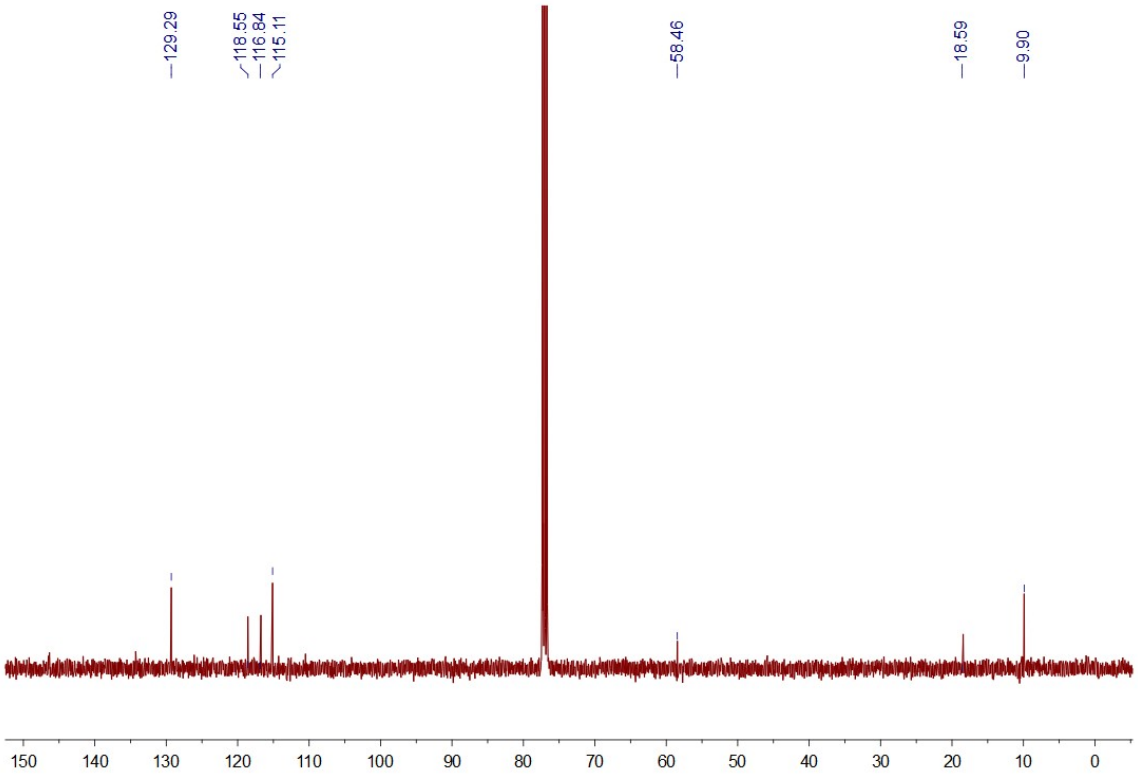

Figure S4. ^{13}C NMR spectrum (100 MHz, $CDCl_3$, 298 K) of compound **2**.

Synthesis of compound **3**: compound **2** (3.72 g, 18.6 mmol) was dissolved in CAN. K_2CO_3 and ethylene bromoacetate was added and refluxed for 18 hours. The solvent was removed under vacuum. The crude product was purified by column chromatography to yield compound **3**. The ^1H NMR spectrum of compound **3** is shown in Figure S5 and the ^{13}C NMR spectrum is shown in Figure S6. ^1H NMR (400 MHz, $CDCl_3$, 298 K) δ (ppm): 7.19 (t, J = 7.6 Hz, 2H), 6.75 (t, J = 7.2 Hz, 1H), 6.62 (d, J = 7.6 Hz, 2H), 4.60 (s, 1H), 3.90 (s, 1H), 2.17 (s, 2H). ^{13}C NMR (100 MHz, $CDCl_3$) δ (ppm): 169.69, 167.37, 129.47, 128.86, 121.79, 68.10, 61.95, 60.98, 50.52, 14.13, 9.74.

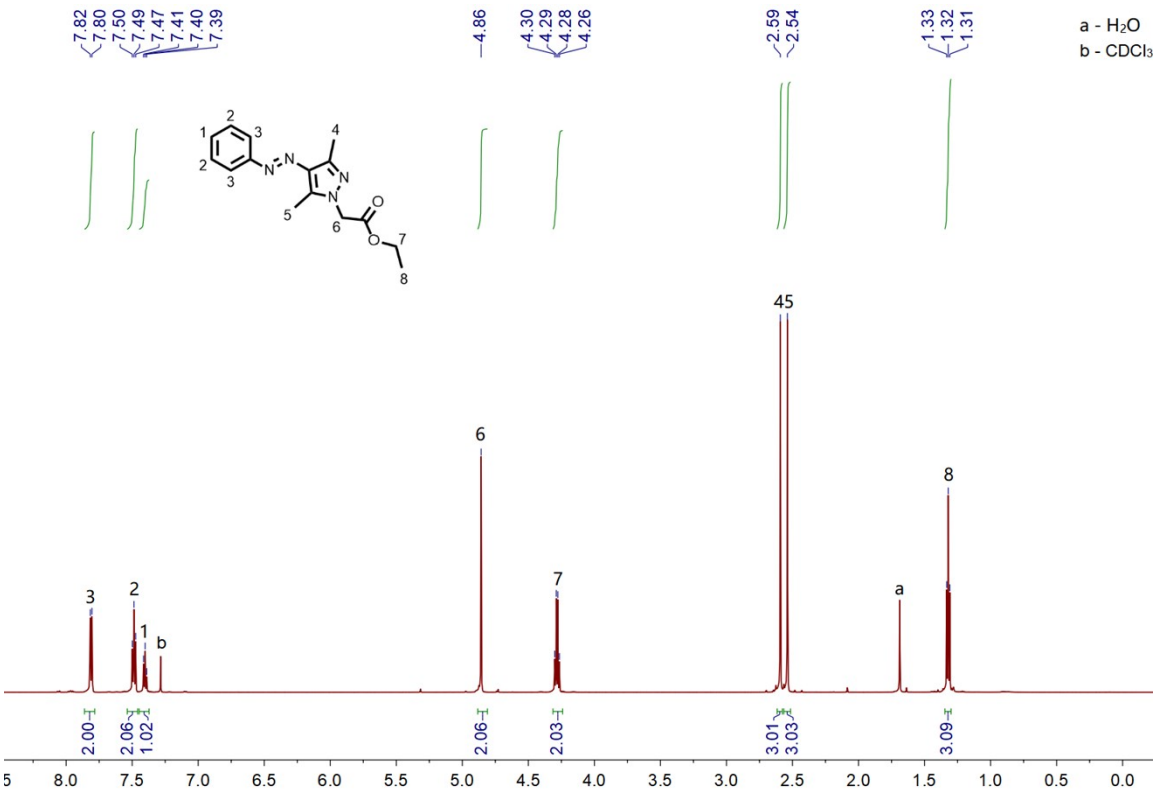

Figure S5. ^{1}H NMR spectrum (400 MHz, $CDCl_3$, 298 K) of compound **3**.

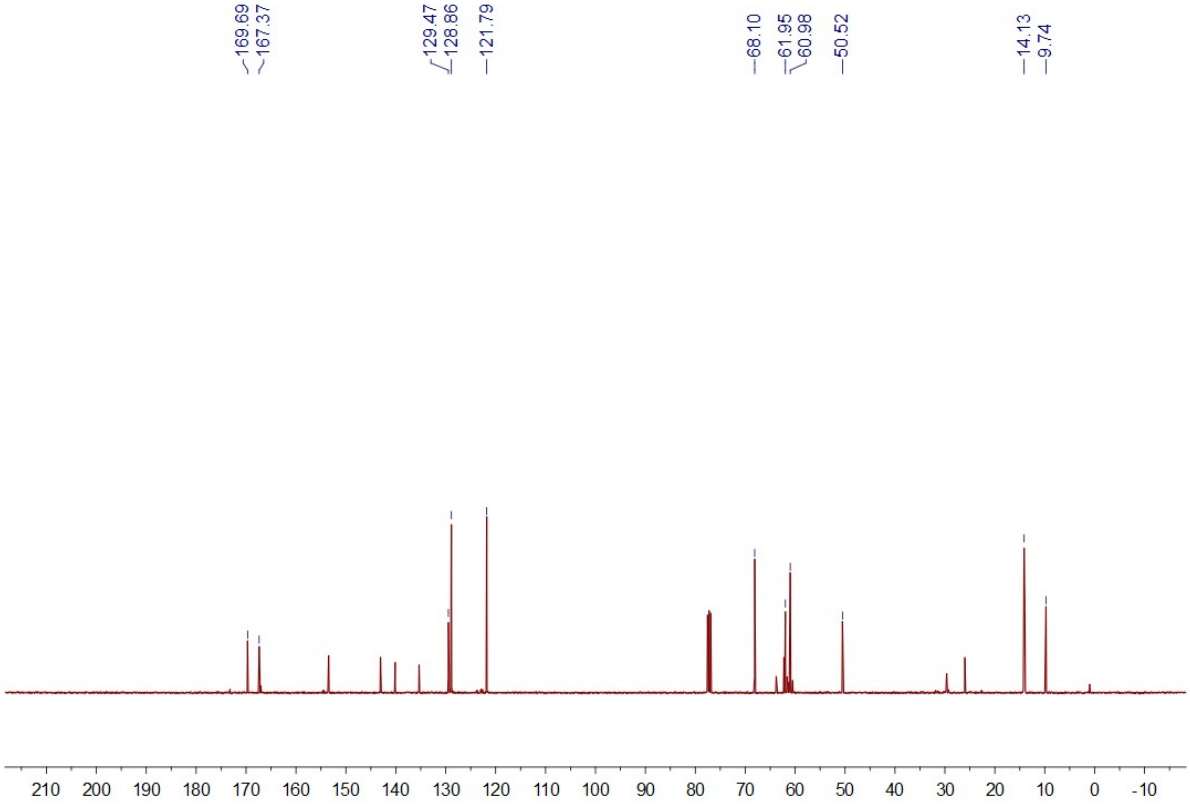

Figure S6. ^{13}C NMR spectrum (100 MHz, $CDCl_3$, 298 K) of compound **3**.

Synthesis of compound **4**: compound **3** (2.13g, 7.44 mmol) was dissolved in THF/water (4:1) and then NaOH (0.45 g, 7.44 mmol) was added. The solution was stirred at room temperature for 18 hours. After removing THF under reduced pressure, the aqueous phase was extracted with EtOAC and the organic layer was discarded. The water phase was acidified with hydrochloride acid. The product **4** was obtained after filtration. The ^{1}H NMR spectrum of **4** is shown in Figure S7. ^{1}H NMR (400 MHz, DMSO-d_6, 298 K) δ(ppm): 7.74-7.72 (d, J = 8 Hz, 2H), 7.53-7.50 (t, J = 6 Hz, 2H), 7.44-7.40 (t, J = 8 Hz, 2H), 4.47 (s, 2H), 2.50 (s, 3H), 2.38(s, 3H). The ^{13}C NMR spectrum of **4** is shown in Figure S8. ^{13}C NMR (100 MHz, DMSO-d_6, 298 K) δ(ppm): 169.78, 153.49, 140.98, 140.79, 134.99, 129.65, 121.85, 52.21, 14.35, 9.95.

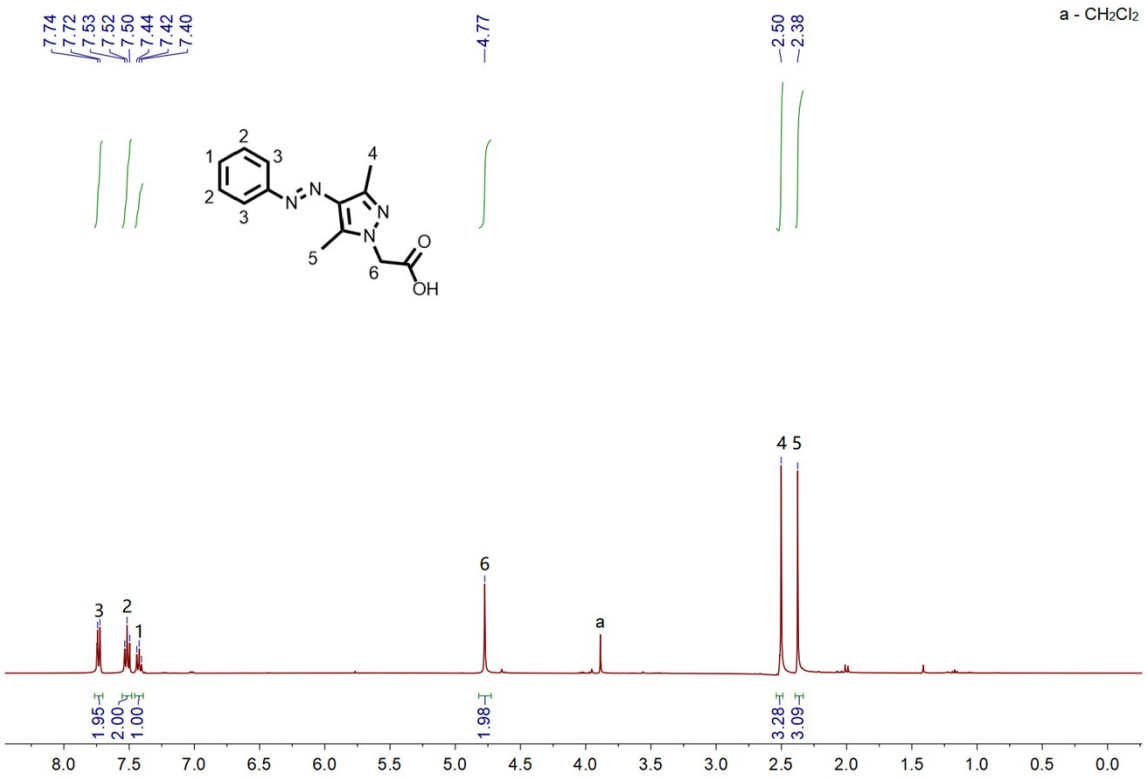

Figure S7. ^{1}H NMR spectrum (400 MHz, DMSO-d_6, 298 K) of compound **4**.

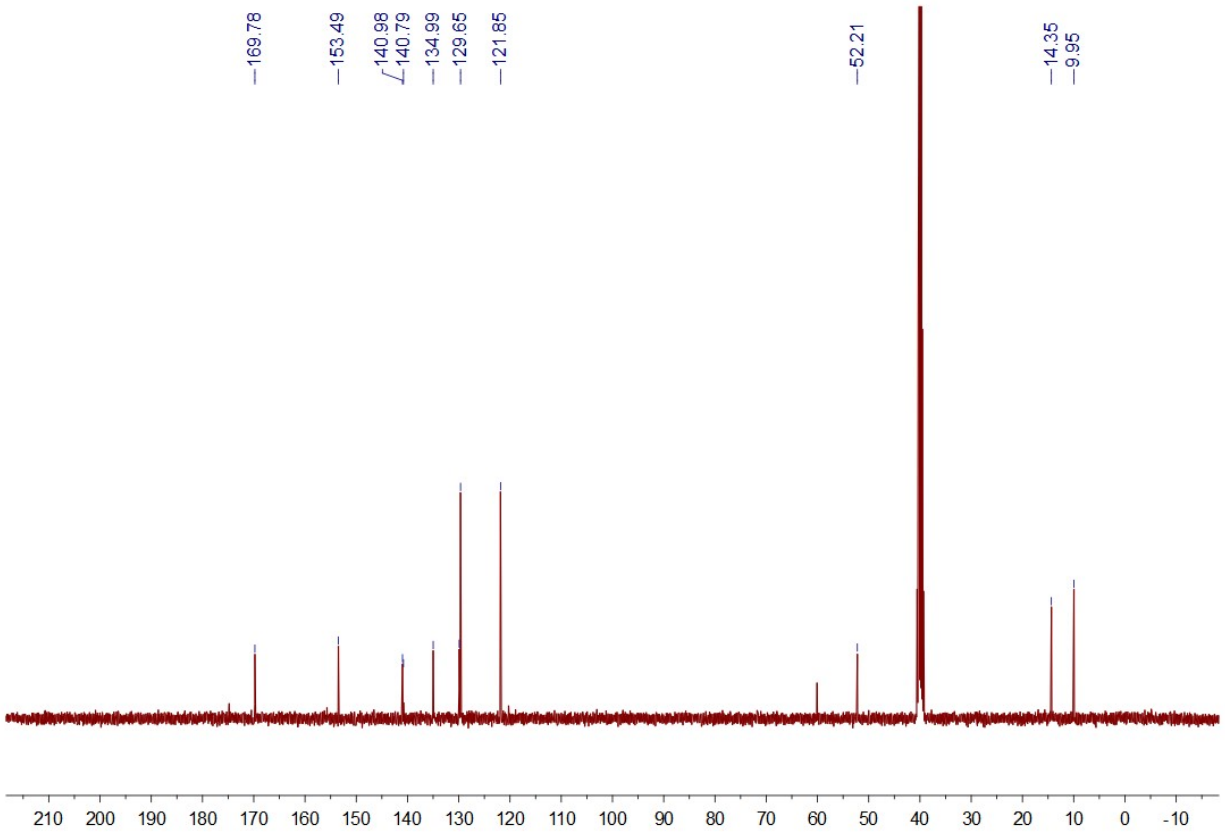

Figure S8. ^{13}C NMR spectrum (100 MHz, DMSO-d_6, 298 K) of compound **4**.

Synthesis of compound **AAP1**: compound **4** was stirred in excess ammonia under reflux for 24 h. The resulting solution was dried in rotavapor and then vacuum-dried for 24 h. The ^{1}H NMR spectrum of **AAP1** is shown in Figure S9 and the ^{13}C NMR spectrum is shown in Figure S10. ^{1}H NMR spectrum spectrum (400 MHz, D_2O, 298 K)δ (ppm): 7.72-7.71 (d, J = 4 Hz, 2H), 7.52-7.48 (t, J = 8 Hz, 2H), 7.45-7.42 (t, J = 6 Hz, 2H), 4.62 (s, 2H), 2.44 (s, 3H), 2.38(s, 3H). ^{13}C NMR (100 MHz, D_2O, 298 K) δ (ppm): 174.30, 152.71, 142.56, 140.44, 134.39, 129.16, 121.34, 52.04, 12.58, 9.04.

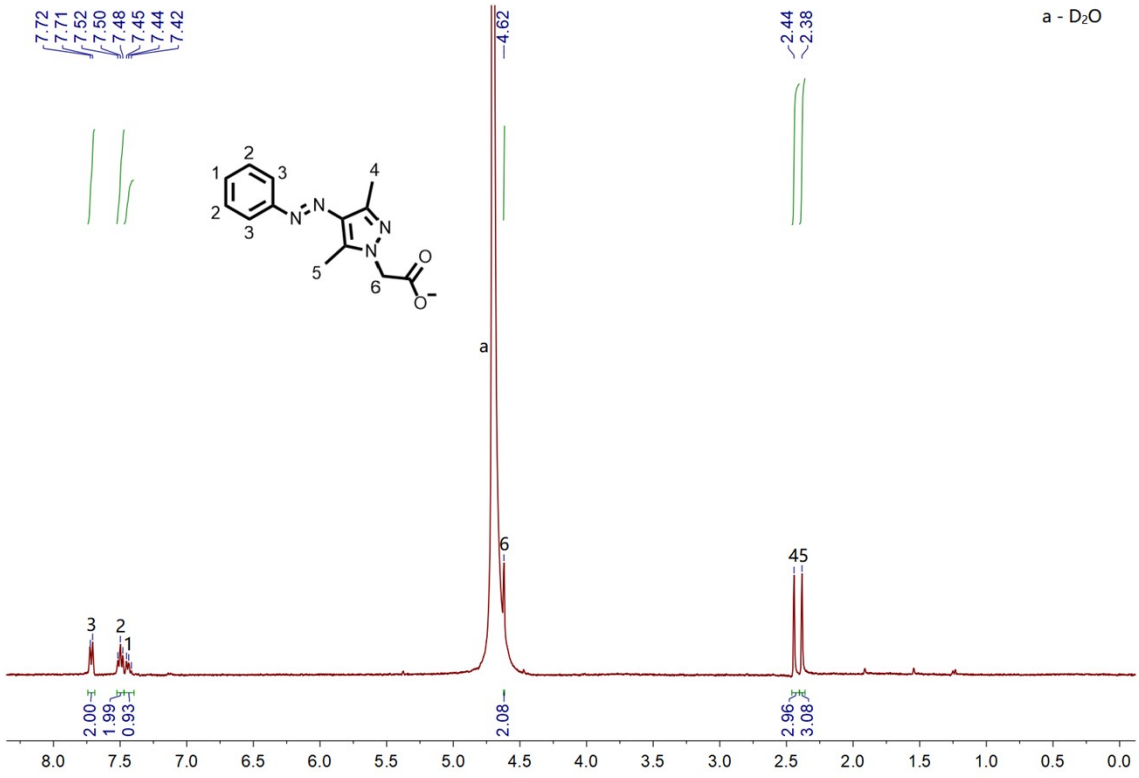

Figure S9. ^{1}H NMR spectrum (400 MHz, D_2O, 298 K) of compound **AAP1**.

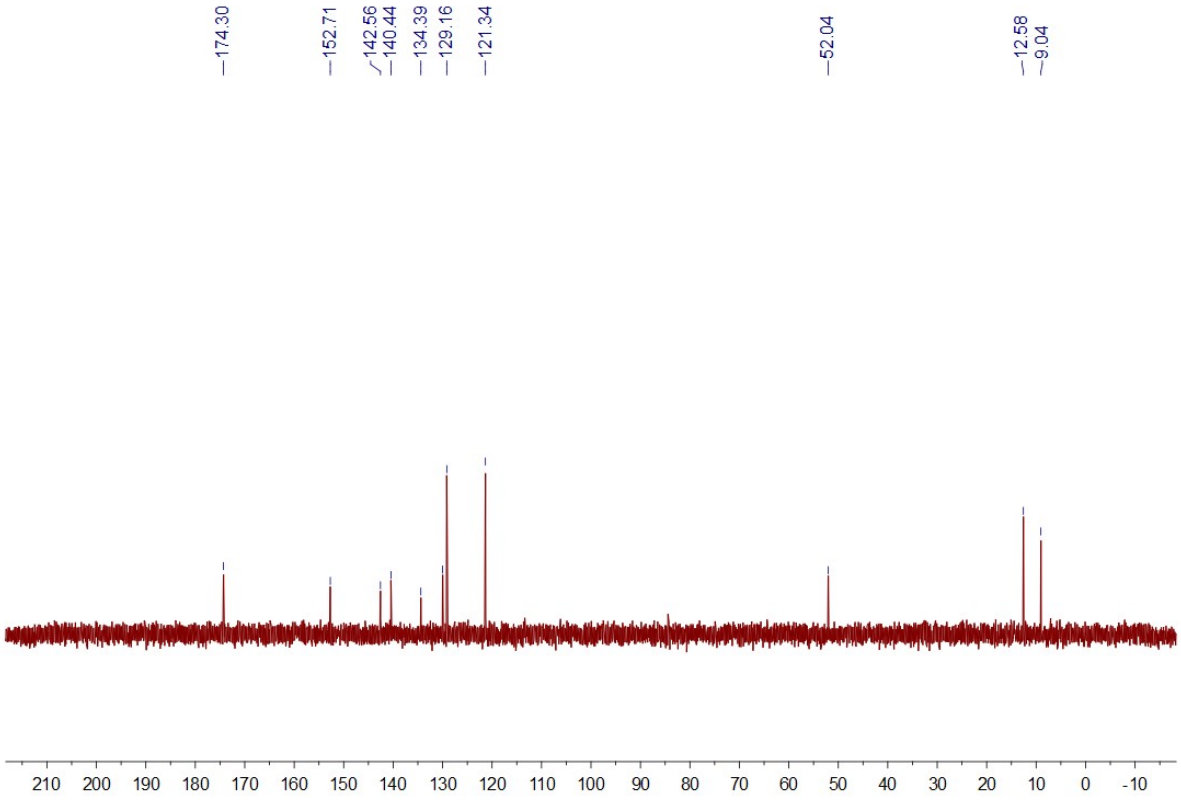

Figure S10. ^{13}C NMR spectrum (400 MHz, D_2O, 298 K) of compound **AAP1**.

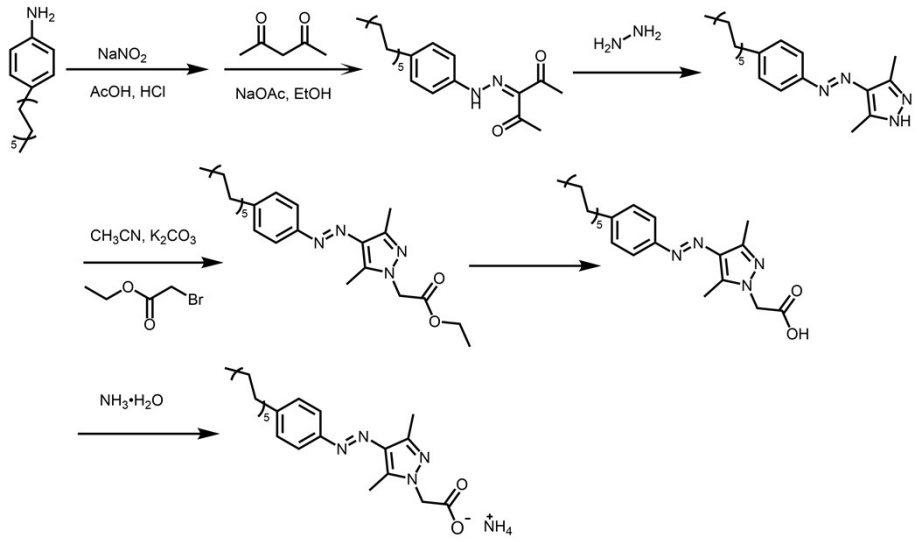

Scheme 2. The synthetic route of compound **AAP2**.

Synthesis of compound **AAP2**: **AAP2** was prepared and purified according to preparation method of **AAP1**, except by changing aminobenzene to P-dodecyl aniline in ***Scheme 2***. The ^{1}H NMR spectrum of **AAP2** is shown in Figure S11 and the ^{13}C NMR spectrum is shown in S12. ^{1}H NMR spectrum (400 MHz, D_2O, 298 K)δ(ppm): 7.74-7.72 (d, J = 8 Hz, 2H), 7.29-7.27 (d, J = 8 Hz, 2H), 4.85 (s, 2H), 2.70-2.66 (t, J = 8 Hz 2H), 2.58 (s, 3H), 2.53(s, 3H), 1.70-1.63 (m, 1H), 1.28(s, 18H), 0.92-0.88(t, J = 8 Hz, 3H). ^{13}C NMR (101 MHz, $CDCl_3$) δ(ppm): 167.46, 151.79, 144.88, 143.29, 139.53, 135.40, 128.92, 121.76, 77.35, 77.04, 76.72, 62.03, 50.61, 35.81, 31.93, 31.43, 29.68, 29.60, 29.52, 29.36, 29.29, 22.70, 14.13, 13.98, 9.84.

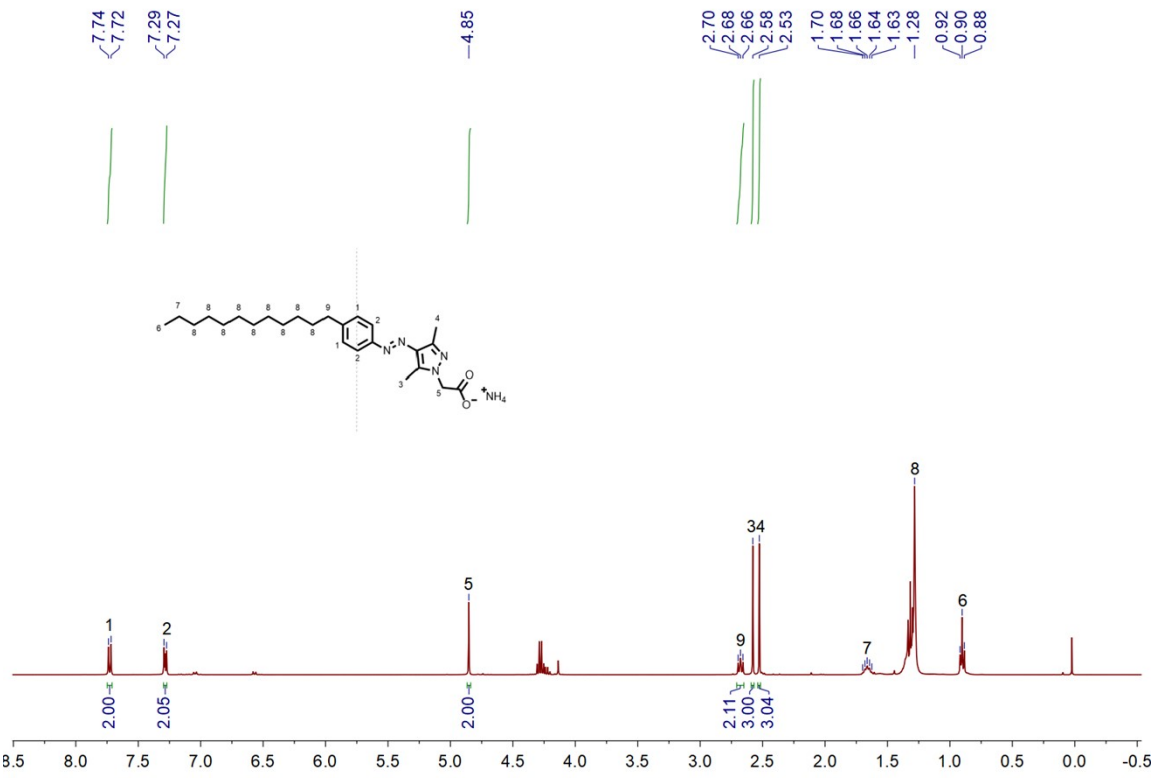

Figure S11. ^{1}H NMR spectrum (400 MHz, DMSO-d_6, 298 K) of compound **AAP2**.

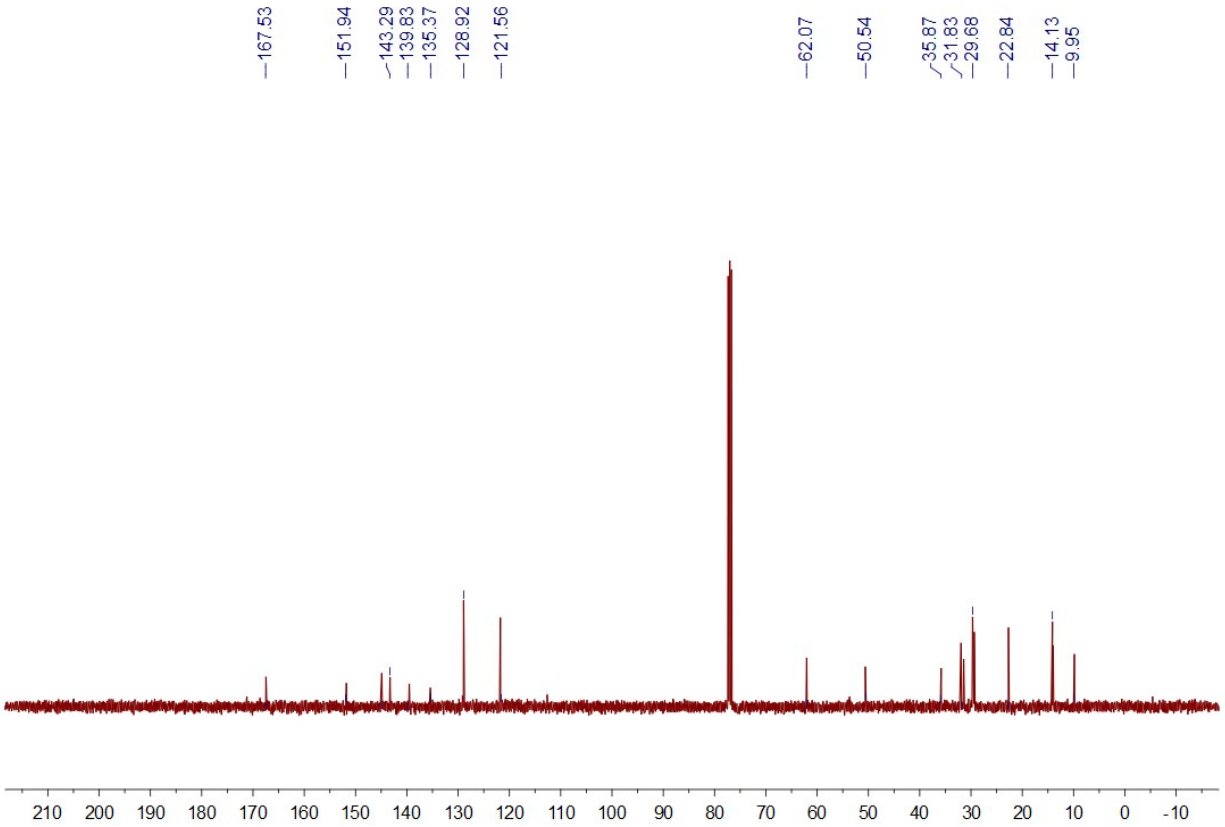

Figure S12. ^{13}C NMR spectrum (100 MHz, DMSO-d_6, 298 K) of compound **AAP2**.

*3. Photo isomerization of trans-**AAP1** and trans-**AAP2***

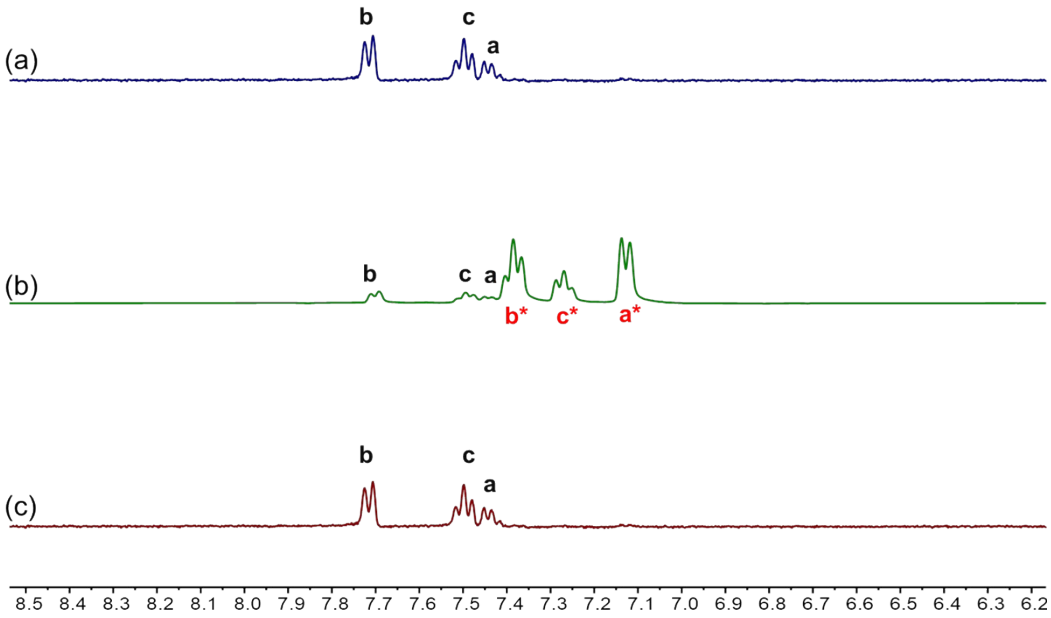

Figure S13. Partial ^{1}H NMR spectrum (400 MHz, D_2O, 298 K) of: (a) 1.0 mM *trans*-**AAP1**; (b) 1.0 mM *trans*-**AAP1** after irradiation with 365 nm UV light for 1 min; (c) (b) after further irradiation with 520 nm green light for 1 min. Based on signal integration, the conversion rate for *trans*- to *cis*- form is estimated to be 89%, *cis*- to *trans*- isomerisation rate is nearly 100%.

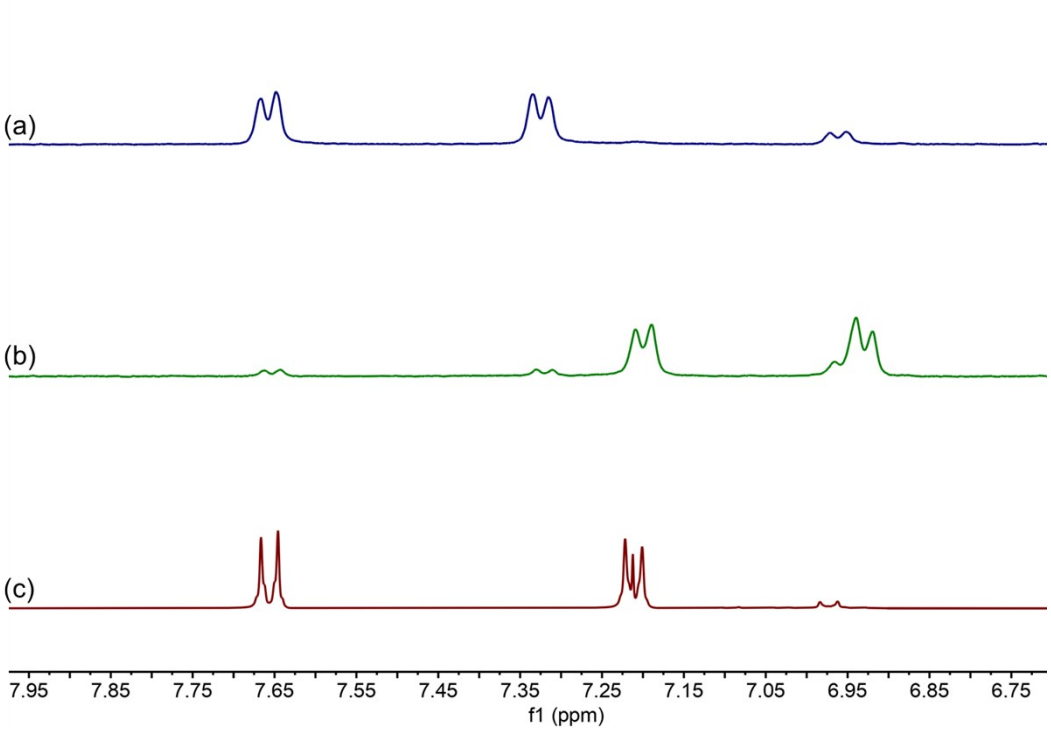

Figure S14. Partial ^{1}H NMR spectrum (400 MHz, D_2O, 298 K) of: (a) 1.0 mM *trans*-**AAP2**; (b) 1.0 mM *trans*-**AAP2** after irradiation with 365 nm UV light for 1 min; (c) (b) after further irradiation with 520 nm

green light for 1 min. Based on signal integration, the conversion rate for *trans*- to *cis*- form is estimated to be 90%, *cis*- to *trans*- isomerisation rate is nearly 100%.

4. *2D NOESY NMR spectroscopy investigation of* ***CWP6*** ⊃*trans-****AAP1***

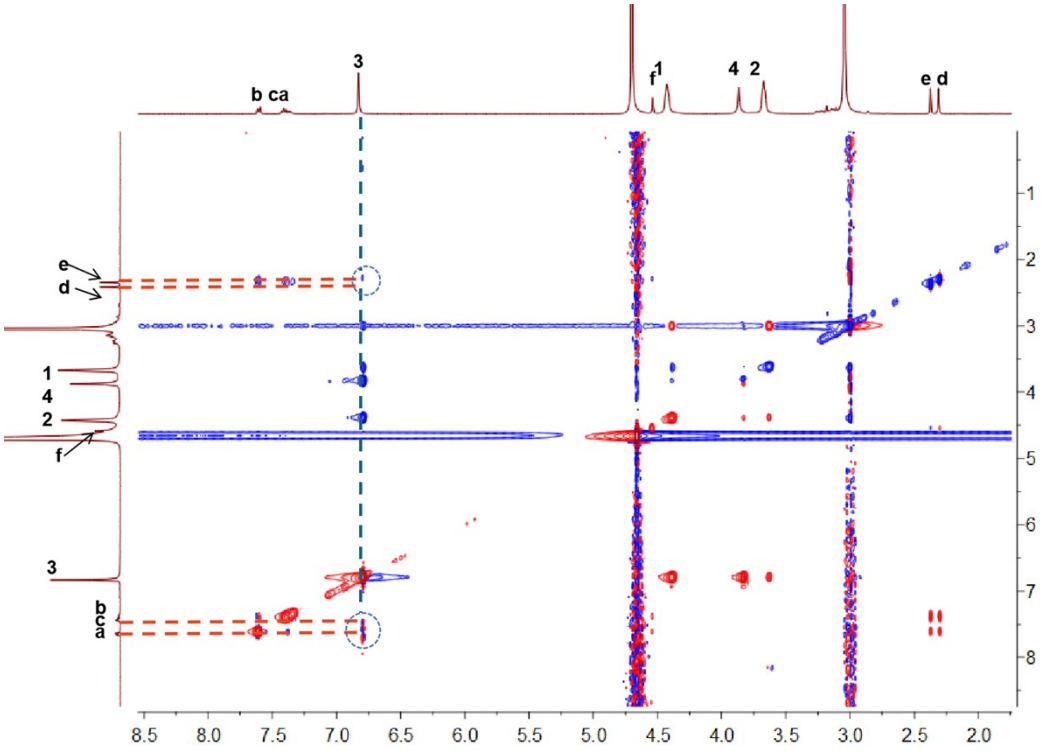

Figure S15. Partial 2D NOESY NMR spectrum (400 MHz, D_2O, 298 K) of **CWP6** (1.0 mM) and *trans*-**AAP1** (1.0 mM).

*5. ^{1}H NMR titration experiments of **CWP6**⊃trans-**AAP1***

To determine the stoichiometries and association constants for the complexation between **CWP6** and *trans*-**AAP1**, ^{1}H NMR titrations were done with solutions which had a constant concentration of *trans*-**AAP1** (0.35 mM) and varying concentrations of **CWP6**. By a non-linear curve-fitting method, the association constants (K_a) of **CWP6**⊃*trans*-**AAP1** was estimated to be $(5.26 \pm 0.38) \times 10^4$ M^{-1}. By mole ratio plots, 1:1 stoichiometries was obtained for both the complexation between **CWP6** and *trans*-**AAP1**. The non-linear curve-fittings were based on the equation:

$$\Delta\delta = (\Delta\delta_\infty/[G]_0)\ (0.5\ [H]_0 + 0.5\ ([G]_0+1/K_a) - (0.5\ ([H]_0{}^2 + (2\ [H]_0(1/K_a - [G]_0)) + (1/K_a + [G]_0)^2)^{0.5}))$$

Where $\Delta\delta$ is the chemical shift change of H_b on *trans*-**AAP1** at $[H]_0$, $\Delta\delta_\infty$ is the chemical shift change of H_b when *trans*-**AAP1** is completely complexed, $[H]_0$ is the initial concentration of **CWP6**, and $[G]_0$ is the fixed initial concentration of *trans*-**AAP1**.

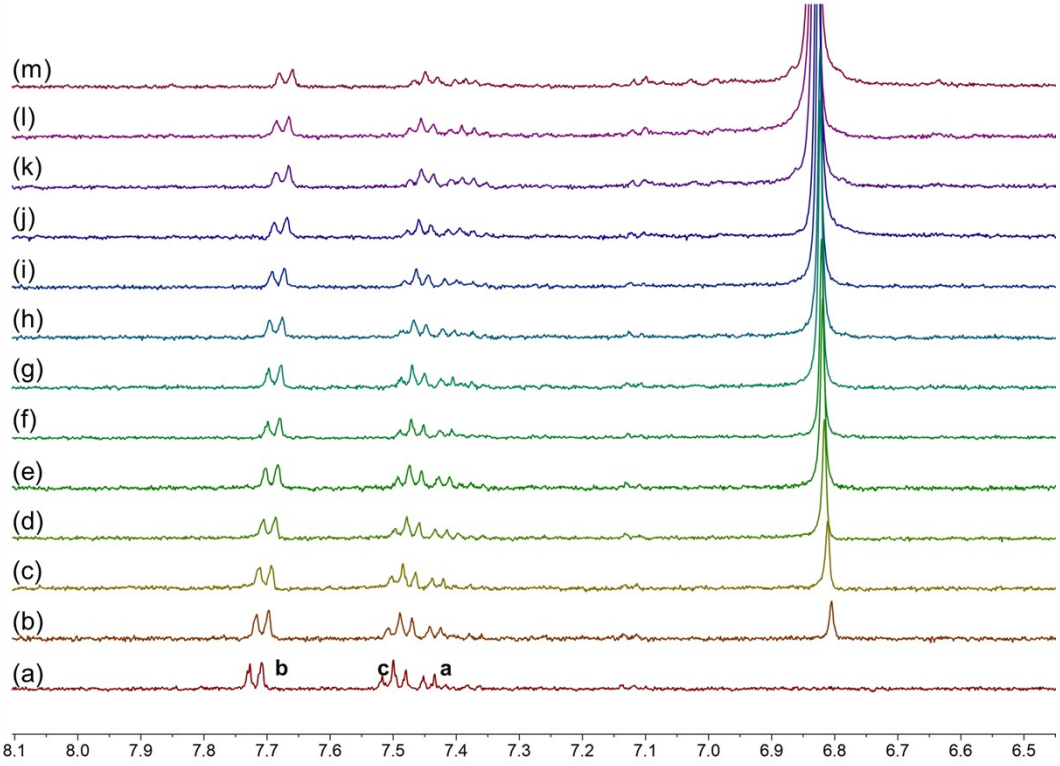

Figure S16. ^{1}H NMR spectrum (400 MHz, D_2O, 298 K) of *trans*-**AAP1** at a concentration of 0.035 mM upon different concentrations of **CWP6**: (a) 0.0 mM, (b) 0.035 mM, (c) 0.068 mM, (d) 0.134 mM, (e) 0.198 mM, (f) 0.260 mM, (g) 0.318 mM, (h) 0.375 mM, (i) 0.534 mM, (j) 0.722 mM, (k) 1.050 mM, (l) 1.400 mM, (m) 1.740 mM.

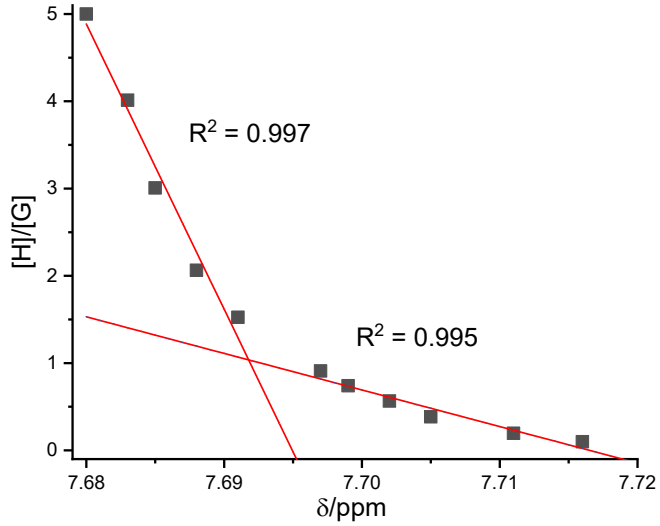

Figure S17. Mole ratio plot for the complexation between **CWP6** and *trans*-**AAP1**, indicating a 1:1 stoichiometry.

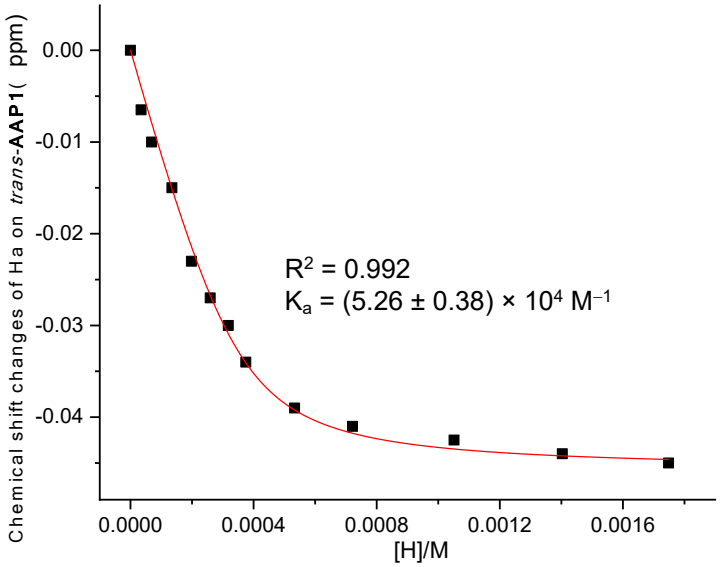

Figure S18. The chemical shift changes of H_b on *trans*-**AAP1** upon addition of **CWP6**. The red solid line was obtained from the non-linear curve-fitting using the above equation.

*6. Critical aggregation concentration determination of trans-**AAP2** and **CWP6**⊃trans-**AAP2***

Some parameters such as the conductivity, osmotic pressure, fluorescence intensity and surface tension of the solution change sharply around the critical aggregation concentration. The dependence of the solution conductivity on the solution concentration is used to determine the critical aggregation concentration. Typically, the slope of the change in conductivity versus the concentration below CAC is steeper than the slope above the CAC. Therefore, the junction of the conductivity-concentration plot represents the CAC value. To measure the CAC value of *trans*-**AAP2** (or **CWP6**⊃*trans*-**AAP2**), the conductivities of the solutions at different concentrations were determined. By plotting the conductivity versus the concentration, we estimated the CAC value of *trans*-**AAP2** (or **CWP6**⊃*trans*-**AAP2**).

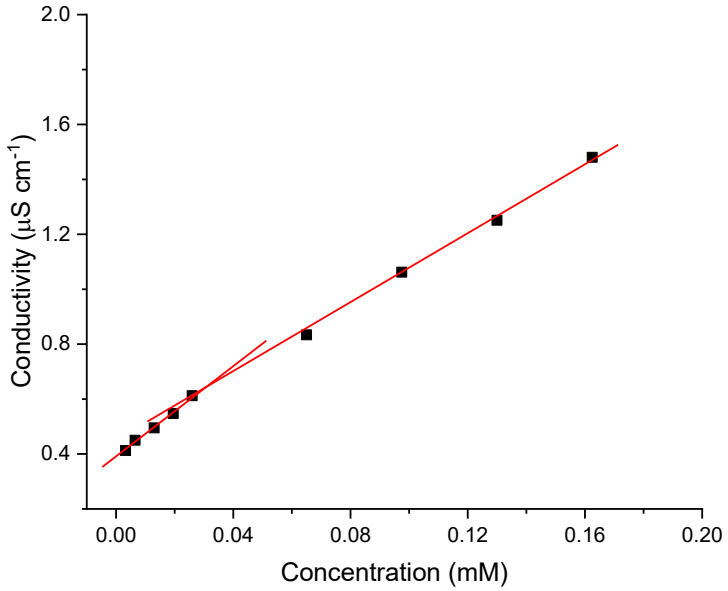

Figure S19. The concentration-dependent conductivity of *trans*-**AAP2**. The critical aggregation concentration (CAC) was determined to be 3.19×10^{-5} M.

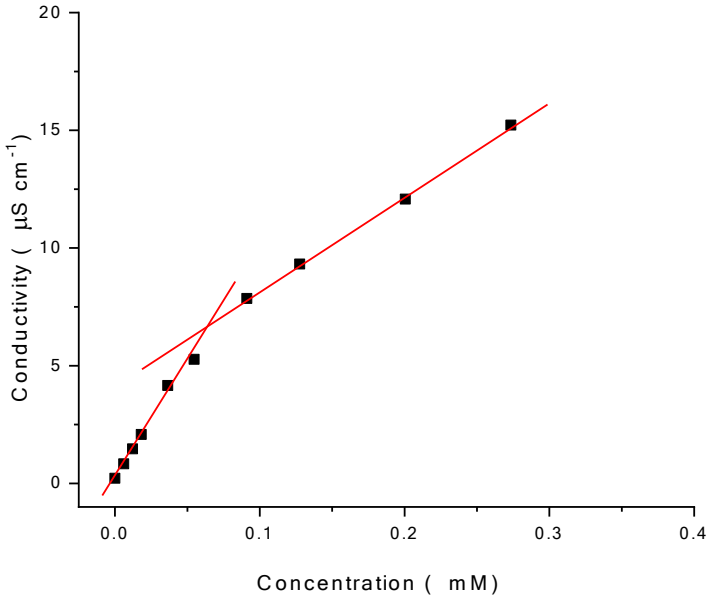

Figure S20. The concentration-dependent conductivity of **CWP6**⊃*trans*-**AAP2**. The critical aggregation concentration (CAC) was determined to be 6.35×10^{-5} M.

7. TEM images

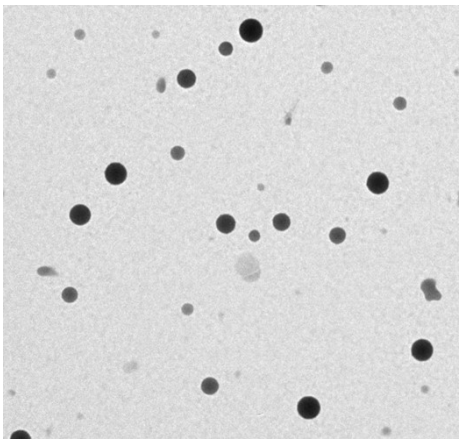

Figure S21. TEM image of *trans*-**AAP2** after UV irradiation.

8. References:

S1. Y. Ma, X. Ji, F. Xiang, X. Chi, C. Han, J. He, Z. Abliz, W. Chen and F. Huang, *Chem. Commun.*, 2011, **47**, 12340–12342.

S2. Y. Ma, J. Yang, J. Li, X. Chi and M. Xue, *RSC Adv.*, 2013, **3**, 23953–23956.